ADVANCED FUNCTIONAL MATERIALS
www.afm-journal.de

Engineered Functional Segments Enabled Mechanically Robust, Intrinsically Fire-Retardant, Switchable, Degradable PolyureThane Adhesives

Yijiao Xue, Meng Zhang, Siqi Huo, Zhewen Ma, Mark Lynch, Bryan T Tuten, Ziqi Sun, Wei Zheng, Yonghong Zhou, and Pingan Song**

Adhesives are being used ubiquitously, such as automotive, building, electronics, and beyond. Due to the lack of rational design strategies, they have yet to achieve a performance portfolio: mechanically robust, highly adhesive, fire-retardant, switchable, and sustainable (e.g., biobased, reusable, biodegradable) to ensure their practical applications. Herein, a fire-retardant phosphorus-containing pimaric acid bio-derivative, AD, as functional segments, is rationally engineered to prepare biobased polyurethane (PU) adhesive that realizes such an integrated performance portfolio. Because of dynamic hydrogen-bonding and π–π stacking of polar AD, the as-prepared PU adhesive exhibits an ultrahigh adhesion force of 38.8 N cm^{-1}. As-prepared adhesive can be readily reused benefiting from its good solubility in ethanol and exhibits temperature-responsive switchable adhesion without degraded adhesion. Also, the adhesive shows intrinsic fire retardance due to its biphasic modes of action. The labile ester bonds in the structure enable the adhesive to completely degrade in the presence of lipase or dilute acid. Further demonstration of its promising applications as an adhesive for nanocomposite heat dissipators shows superior dissipating efficiencies to commercial heat sinks. This work offers a novel design approach for creating next-generation sustainable high-performance adhesives with functional integration and circular life cycles, which are anticipated to find extensive real-world applications.

1. Introduction

Adhesives are applied to bond different components into semifinished or finished products by utilizing chemical and/or physical interactions. This has enabled them to be a ubiquitous technology used extensively in industry.[1] Recently, there is an increasing demand for adhesives with an integrated performance portfolio of high adhesion strength, high ductility, fire retardance, and sustainability, such as biobased, biodegradability, and reusability for next-generation high-performance adhesives. Such a performance portfolio has become a prime target for practical applications in the automotive, furniture, construction and building, electronics, and, aerospace fields.[2] Despite some encouraging advances, current commercially available and reported adhesives only show one or two of the above performance properties.

Thermoplastic polyurethane (PU) elastomers, comprising both hard and soft segments in the main chain, consisting of

Y. Xue, M. Zhang, Y. Zhou
Institute of Chemical Industry of Forest Products
Chinese Academy of Forestry (CAF)
Nanjing 210042, China
E-mail: zyh@icifp.cn

S. Huo
Centre for Future Materials
School of Engineering
University of Southern Queensland
Springfield 4300, Australia

Z. Ma, W. Zheng
Department of Polymer Materials
School of Materials Science and Engineering
Tongji University
Shanghai 201804, China

M. Lynch, P. Song
Centre for Future Materials
School of Agriculture and Environmental Science
University of Southern Queensland
Springfield 4300, Australia
E-mail: Pingan.Song@usq.edu.au

B. T Tuten, Z. Sun
Centre for Materials Science
School of Chemistry and Physics
Queensland University of Technology
Brisbane QLD 4000, Australia

The ORCID identification number(s) for the author(s) of this article can be found under https://doi.org/10.1002/adfm.202409139

DOI: 10.1002/adfm.202409139

intra and intermolecular hydrogen-bonding (H-bonding) within and between chains, often simultaneously produces high bonding strength and fracture toughness, and thus hold great potential as high-performance adhesives.[3] In addition, thermoplastic PU elastomers show high solubility in most polar solvents, which facilitates their recycling. Unfortunately, high flammability and poor biodegradability have been challenging for PU elastomers that limits their real-world applications in industry. Recent advances in fire-retardant PU elastomers are achieved by introducing additive fire retardants (FRs) or by chemically bonding fire-retardant groups.[4] Additive FRs, often produce deteriorated mechanical properties in PU due to poor polymer-FR interfacial compatibility and/or high loading levels of FRs, though satisfactory fire retardance is usually achieved. In contrast, the chemical bonding of fire-retardant groups into PU polymer chains is a better option as it can impart desirable fire retardancy without compromising other performances of the resulting PU.[5] As a typical example, a vanillin-derived PU elastomer was recently reported to show a high limit oxygen index (LOI) value of 32.8% and a satisfactory UL-94 V-0 rating, a large break strain of 2260% and a record-high toughness (ca. 460 MJ m^{-3}), attributed to the inclusion of dynamic π–π stacking motifs and phosphorus-containing moieties.[6] In another study, the designed PU elastomer nanocomposite containing a small amount of cellulose nanocrystals showed a self-extinguishing ability (a UL-94 V-0 rating) with an anti-dripping behavior, that can be completely degraded in lipase solution at 37 °C in 60 days.[7] Despite excellent fire retardant, mechanical and degradable properties, both of the PU elastomers do not have acceptable adhesion abilities, and thus cannot be used as adhesives. Additionally, a fire-retardant PU adhesive or sealant was recently fabricated by introducing a phosphorus and nitrogen-containing PU prepolymer, but the adhesive properties are yet to be characterized, though it does show unsatisfactory mechanical properties.[8] Therefore, it remains a major challenge to create mechanically robust, fire-retardant PU adhesives.

Sustainability has increasingly become another key requirement for adhesives in terms of the source of raw materials, biodegradability, and reusability. This is particularly vital in the current context of the accelerated depletion of fossil resources, and rapid accumulation of micro/nanoplastics in the environment. To this end, various biological derived chemicals, such as vanillin, dopamine, and abietic acid have been used as functional components in the hard segments of PUs,[6,7,9] and many chain-shattering biodegradable polyesters, such as polylactide (PLA), polycaprolactone diol (PCL),[10] poly(butyleneadipate-co-terephthalate) (PBAT),[11] and poly(butylene succinate) (PBS),[12] have been employed as biodegradable soft building blocks for PUs because of their high sensitivity to many types of agents. Additionally, materials containing labile ester bonds show great promise as degradable hard segments for PU.[13]

Herein, we rationally designed a biobased acrylic pimaric acid-based PU adhesive that exhibits a desirable performance portfolio, including mechanical robustness, strong adhesion strength, intrinsic fire retardance, complete recycling, and degradability. The resulting PU adhesive shows a strong peel strength (up to 38.8 N cm^{-1}) on a polyvinyl chloride (PVC) substrate. It can be reused using ethanol and easily de-bonded on-demand by changing temperatures. As-synthesized PU adhesive can extinguish the flame upon flame removal. In addition, the PU adhesive completely breaks down in lipase or acetic acid solutions, showing excellent biodegradability and chemical degradability. We further demonstrate its application as a thermal dissipator film by blending it with copper powders. This film exhibits a better heat dissipation capacity than commercial silicone greases. This work is a promising strategy for the creation of the next-generation of sustainable functional adhesives, which will broaden their practical application in electronics, furniture, building and construction, automobile, and many other sectors.

2. Results and Discussion

2.1. Design and Characterization of Fire-Safe and Sustainable PU Adhesive

To create fire-retardant sustainable PU elastomer adhesives, a 9,10-dihydro-9-oxa-10-phospaphenantrene-10-oxide (DOPO) derivative, DHDP was selected as the fire retardant moiety because of its high efficiency. A rosin-derived acrylic pimaric acid (APA) was selected as a biodegradable building block for achieving strong adhesion due to its carboxyl groups and unique phenanthrene aggregation structure. Then a rationally designed P/N-containing biobased diols, AD (see section 1.2 Supporting Information), were prepared between DHDP and APA to serve as the hard segments to synthesize the target PU elastomer adhesives (PU-AD). Polytetramethylene glycol (PTMEG, M_n = 2000 g mol^{-1}) was used as a soft segment (see **Figure 1a**). It is worth noting that in this molecular design, the π–π interactions in the DHDP structure were expected to not only promote adhesion of the target PU adhesives by increasing the interchain cohesive energy, but also to improve the mechanical properties of the adhesive through physical crosslinking.

To investigate this synergistic adhesion between APA and DHDP groups, two control PU elastomers, PU-AEG with only APA (Figure S1, Supporting Information) and PU-DHDP with only DHDP in their hard segments were synthesized (Figure 1b; Section 1.2 Supporting Information). The chemical structures of both AD and AEG were confirmed by infrared spectroscopy (IR), ^{1}H-Nuclear Magnetic Resonance (^{1}H NMR) and ^{31}P NMR analysis. In the IR spectra, the disappearance of characteristic carbonyl groups and the appearance of ester and hydroxy groups indicates the successful synthesis of AD and AEG (Figure S3, Supporting Information). In addition, the corresponding chemical shifts of ^{1}H and ^{31}P in the NMR spectra -further supports their successful synthesis (Figure S4–S6, Supporting Information). The elemental composition of AD is consistent with theoretical values, with a P content as high as ≈6.5 wt% (Table S2, Supporting Information). The chemical structures of three PU elastomers, PU-AD, PU-AEG, and PU-DHDP, were confirmed by IR spectra as well, as evidenced by the disappearance of characteristic peaks of NCO groups (Figure S7, Supporting Information). The three PU elastomers show number-average molecular weights (M_n) of 20–40 kDa and weight-average molecular weights (M_w) of 55–90 kDa, with dispersities indicative of step-growth polymerization according to Carother's equation ($Đ > 2.0$) by gel permeation chromatography (GPC) (Table S3, Supporting

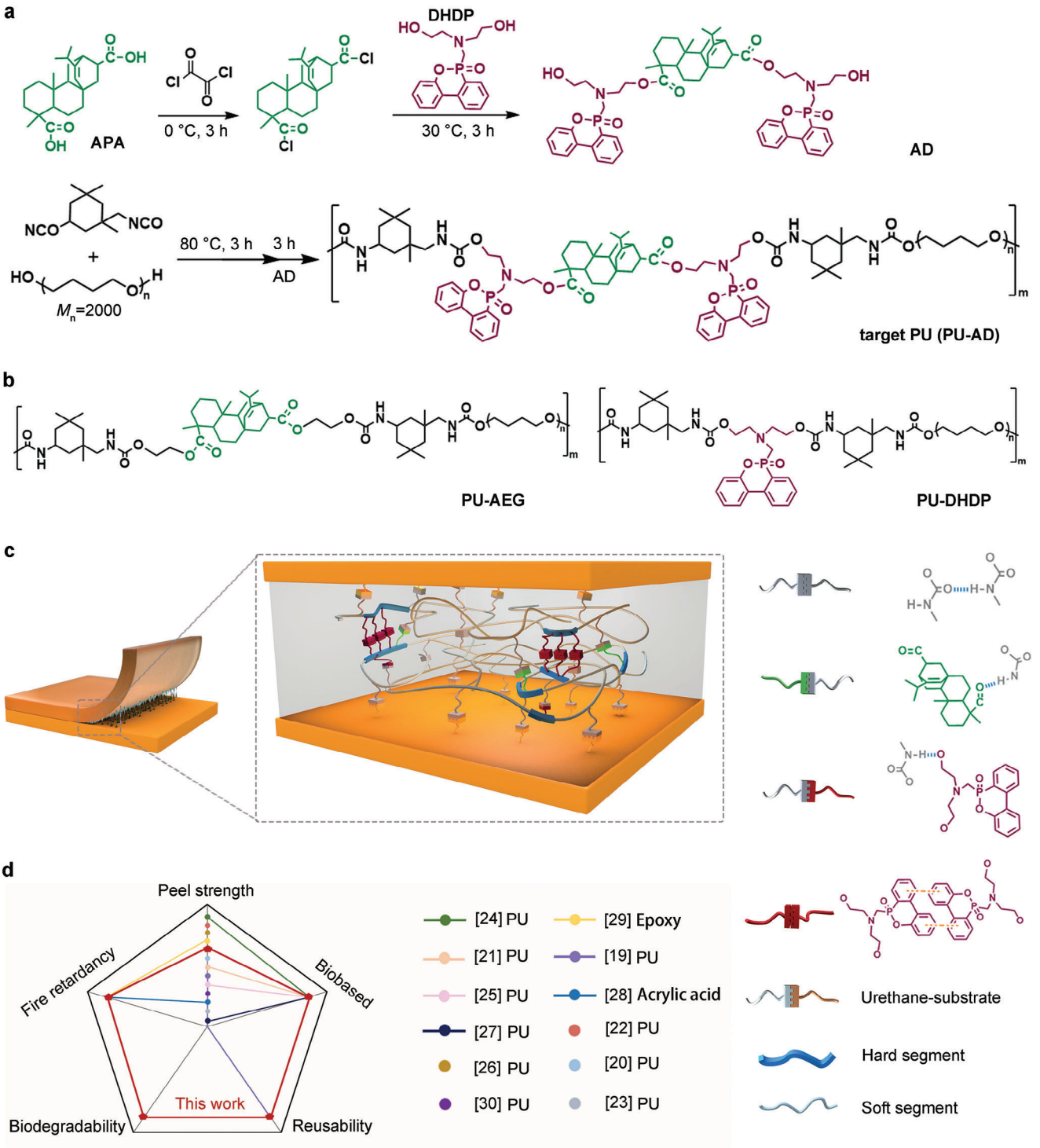

Figure 1. Rational design and characterizations of robust, fire-retardant, switchable, sustainable PU adhesives, PU-AD. a) The synthetic routes of AD and PU-AD. b) Chemical structures of PU-AEG and PU-DHDP elastomers for comparison. c) Structural illustration of PU-AD adhesive. d) Comparison of comprehensive performances of PU-AD with other adhesive counterparts.[14]

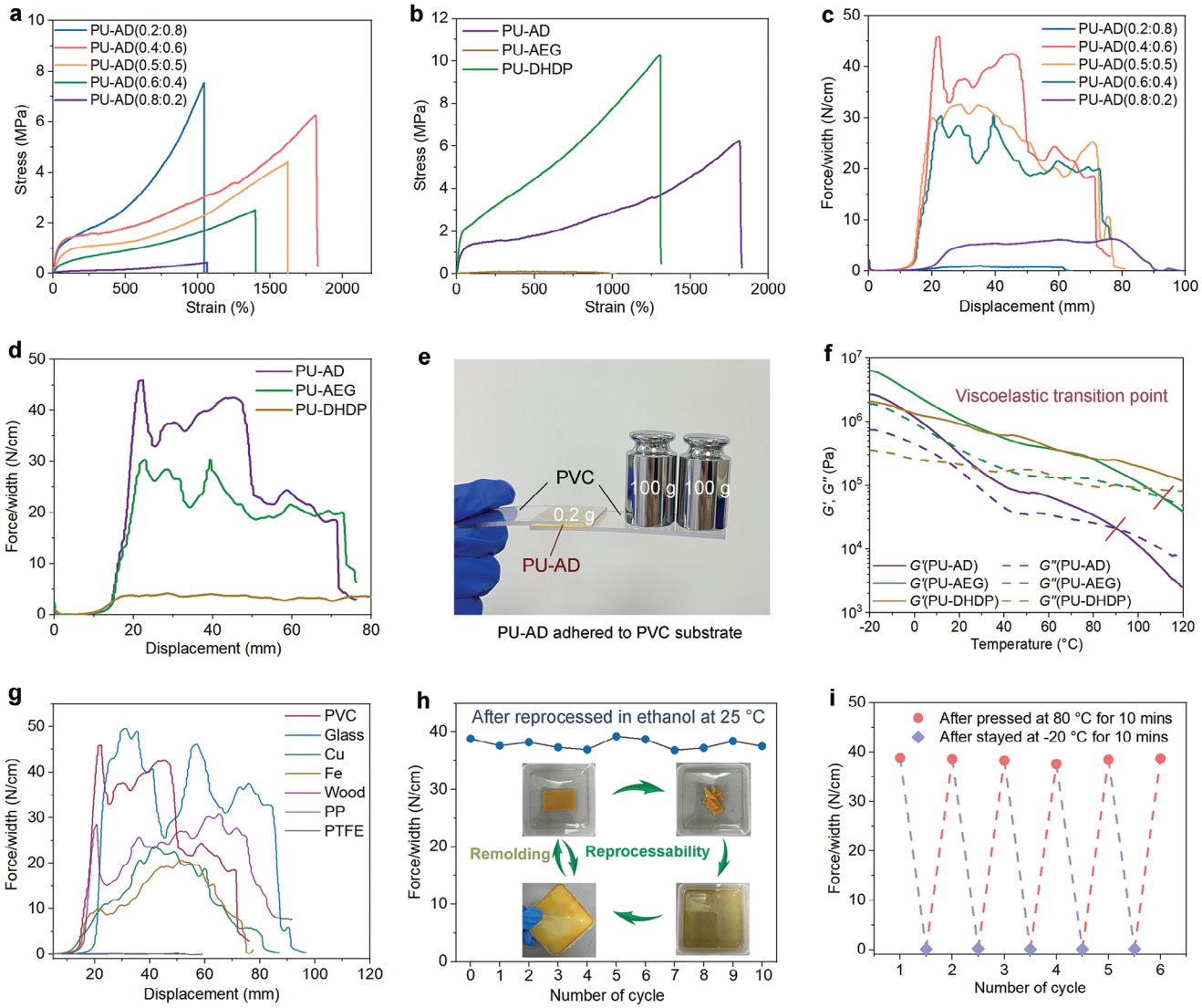

Figure 2. Mechanical and adhesive properties of PU-AD. Typical engineering stress–strain curves of as-synthesized a) PU-AD with different PTMEG/AD ratios and b) PU-AD (0.4:0.6) and other two PU elastomers. Peel curves through the 90° peeling test for the PU-AD elastomers that were adhered to PVC with c) different PTMEG/AD ratios and d) different hard segments. e) Digital pictures exhibiting that the PU-AD possesses excellent adhesion property. f) Temperature dependence of storage modulus (G') and loss modulus (G'') for PU elastomers. g) Peel curves of PU-AD (0.4:0.6) adhered to different substrates. h) Peel strength of PU-AD (0.4:0.6) after reprocessing in ethanol 10 times. i) Five cycles of adhesion between PU-AD (0.4:0.6) and PVC at −20 and 80 °C.

Information). All three PU elastomers show typical microphase-separated structures, as observed by atomic force microscopy (AFM) (Figure S8, Supporting Information). PU-AD exhibits island microphase separated domains (hard segments) with a size of ≈50 nm in width uniformly dispersed in the continuous matrix (soft segments) (Figure S8a, Supporting Information). For PU-DHDP, the size of the island is ≈100 nm, larger than that of PU-AD (Figure S8c, Supporting Information), suggesting a higher degree of microphase separation in PU-AD due to the presence of rigid structures of both APA and DHDP. From the phase images, the island structure can be observed in both PU-AD and PU-DHDP (Figure S8a$_1$,c$_1$, Supporting Information). However, the phase interface for PU-AEG is blurry and the microphase separation is not obvious in the height image (Figure S8b, b$_1$, Supporting Information), indicating that π–π stacking plays a more important role in inducing the microphase separation of PU-AD and PU-DHDP.

By combining APA and DHDP groups, the target PU-AD exhibits excellent adhesion to a PVC substrate, as can be seen with a thin piece of PU-AD (0.2 g, 0.2 mm thick, 1.5 mm wide) supporting a weight (200 g) 1000 times larger than its own weight without breakage (**Figure 2e**). Such superior adhesive performance is achieved primarily by constructing hard domains through the self-assembly of π–π stacking (red–red) with multilevel H-bonding (grey–grey, green–grey, and grey–red, respectively, representing the interactions between urethane–urethane, APA–urethane, and urethane–DHDP), and by forming effective interfacial adhesion between PU and active components on the

substrate (e.g., grey–yellow representing the interaction between Cl–urethane) (Figure 1c), as well as the polarity of APA groups. As a result, PU-AD exhibits a peel strength as high as 38.8 N cm^{-1} with PVC as substrate, which is superior to other adhesives (Figure 1d).[14] More importantly, the target PU-AD outperforms existing adhesive counterparts in the integrated performance portfolio, including peel strength, fire retardancy, biodegradability, and reusability, while being biobased, which is yet to be achieved in other adhesives (Figure 1d; Table S4, Supporting Information).

2.2. Mechanical and Adhesive Properties

The mechanical properties of the PU elastomers were measured by tensile testing. PU-AD (0.4:0.6) with appropriate fractions of AD hard segments shows the superior balanced tensile stress of 6.2 MPa and strain of ≈1800% (Figure 2a). For contrast, PU-AEG and PU-DHDP with PTMEG/AD ratio at 0.4:0.6 were also prepared. Despite a higher tensile strength of PU-DHDP (10.3 MPa) when compared to PU-AD, an obviously larger break strain of PU-AD was achieved as compared to PU-AEG and PU-DHDP (Figure 2b). The great extensibility of PU-AD is beneficial to large deformation during the peeling process, thus contributing to its higher adhesion performance.[14b] For PU-AEG, it is mechanically weak but still gives a break strain of ≈1000%, which favors its peeling strength.

The 90° peel test was used to assess the adhesion of PU elastomers.[15] The adhesive property of the PU-AD can be readily tailored by tuning the molar ratios of PTMEG and AD (Figure 2c). PU-AD (0.4:0.6) exhibits the highest peel strength of 38.8 N cm^{-1} (Figure S9, Supporting Information), which is higher than PU-AD with other PTMEG/AD ratios. With increasing peeling force, the PU-AD (0.4:0.6) adhesive adjacent to the crack undergoes significant deformation to resist separation from the adhesion interface (Figure S10, Supporting Information), thus resulting in enhanced adhesion. Note, to facilitate the investigation of the adhesion and fire-retardant effects of APA and DHDP, a soft/hard segment molar ratio of 0.4:0.6 was used to synthesize PU-AEG and PU-DHDP. Three PU adhesives show a peel strength in the order of PU-AD (38.8 N cm^{-1}) > PU-AEG (21.2 N cm^{-1}) > PU-DHDP (3.2 N cm^{-1}) (see Figures 2d and S11, Supporting Information). The results verify our assumptions that there exists a synergistic adhesion between APA and DHDP groups through polar structures and H-bonding of APA and π–π stacking of DHDP.[16]

A MD simulation was performed to calculate the interaction energies between PVC substrates and PU adhesives (see section 1.6 Supporting Information),[17] with the theoretical calculations further verifying the experimental results (Figure S2 and Table S1, Supporting Information). Both $E_{PU\text{-}PVC}$ and E_{PU} values for PU-AD ($E_{PU\text{-}PVC}$ = −9375.5, E_{PU} = −6688.8 kcal mol^{-1}) were larger than those of PU-AEG ($E_{PU\text{-}PVC}$ = −6694.4, E_{PU} = −4144.7 kcal mol^{-1}) and PU-DHDP ($E_{PU\text{-}PVC}$ = −5869.7, E_{PU} = −3310.8 kcal mol^{-1}), and the resulting interaction energy (IAE) value between PU and PVC follows the order of PU-AD > PU-AEG > PU-DHDP, which is consistent with the highest peel strength of PU-AD that can be visually observed in Figure 2e. The bonding force in PU-AD induced by π–π interactions, H-bonding and polar structure is significantly enhanced by the combination of APA and DHDP, which drives the self-assembly and increases the cohesive energy.[18] The rheological testing results (Figure 2f) shows that as the temperature increases, both the storage modulus (G') and loss modulus (G'') drop sharply, which is presumably due to the dissociation of π–π stacking and multiple H-bonds. Also, the viscoelastic transition temperature, which is the intersection point of G' and G'', was determined for three PUs,[14b] which gave results in the order of PU-AD < PU-AEG < PU-DHDP, indicating that PU-AD chains flow faster at the hot press temperature (e.g., 80 °C). This makes it easier for PU-AD chains to spread on the substrate surface, thus increasing their contact area and leading to higher peel strength.

To further demonstrate the adhesion capability of as-engineered PU-AD adhesives, we conducted the peeling test of PU-AD on different substrates (e.g., PVC, glass, Cu, Fe, wood, PP, PTFE) (Figures 2g and S12, Supporting Information). The PU-AD exhibits the highest peel strength on PVC (38.8 N cm^{-1}), then glass (37.9 N cm^{-1}), while the peeling values for wood, Cu and Fe are lower, reaching 25.0, 19.7, and 15.2 N cm^{-1}, respectively. Unfortunately, PU-AD seems to show very limited adhesion to nonpolar PP and PTFE, two difficult-to-stick materials. This means that as-prepared PU-AD shows excellent adhesion to polar materials because of its own polar properties.

2.3. Reusability and Switchable Adhesion

The reusability of PU-AD as an adhesive was evaluated by reversibly dissolving it in ethanol and allowing it to adhere to PVC surfaces. The adhesive strength remains stable without obvious decay after 10 cycles of dissolution and adhesion (Figure 2h). Because a nontoxic solvent with low energy consumption is involved during the reuse process, this makes PU-AD an ideal sustainable adhesive candidate for industry, and is thus superior to previous PU, acrylate, and epoxy adhesives in term of its performance portfolio (Figure 1d; Table S4, Supporting Information).

Generally, it is preferable for an adhesive to show a switchable adhesion or on-demand bonding and debonding abilities without causing any subsequent damage.[19] As-prepared PU-AD adhesive shows a switchable adhesion simply by changing the temperature that can induce reversible adhesion through altering its viscoelastic states. Upon cooling the adhesive to −20 °C for 10 min, the interfacial strength drops down to 0.2 N cm^{-1}; When the temperature is raised to 80 °C and held for 10 min, the adhesive regains its high adhesion, even after five cycles (Figure 2i). Such an on-demand switchable adhesion ability is due to the fact that, at high temperatures, polymer chains can quickly diffuse to the adhered surface, increasing the interfacial contact area due to their low modulus and high chain mobility. The PU-AD can form multiple interfacial interactions with the adhered surface, which is facilitated by H-bonding in the presence of free urethane groups. This can also explain why the peel strength of PU-AD shows an increasing trend when the temperature increases from −20 to 80 °C (Figure S13 and Table S5). Upon cooling to −20 °C, the PU-AD adhesive hardens and further forms intra/intermolecular H-bonds, thus weakening the H-bonding and then adhesion with the interface. As a result, the adhesive exhibits a low peel force during testing.[14a,b,16]

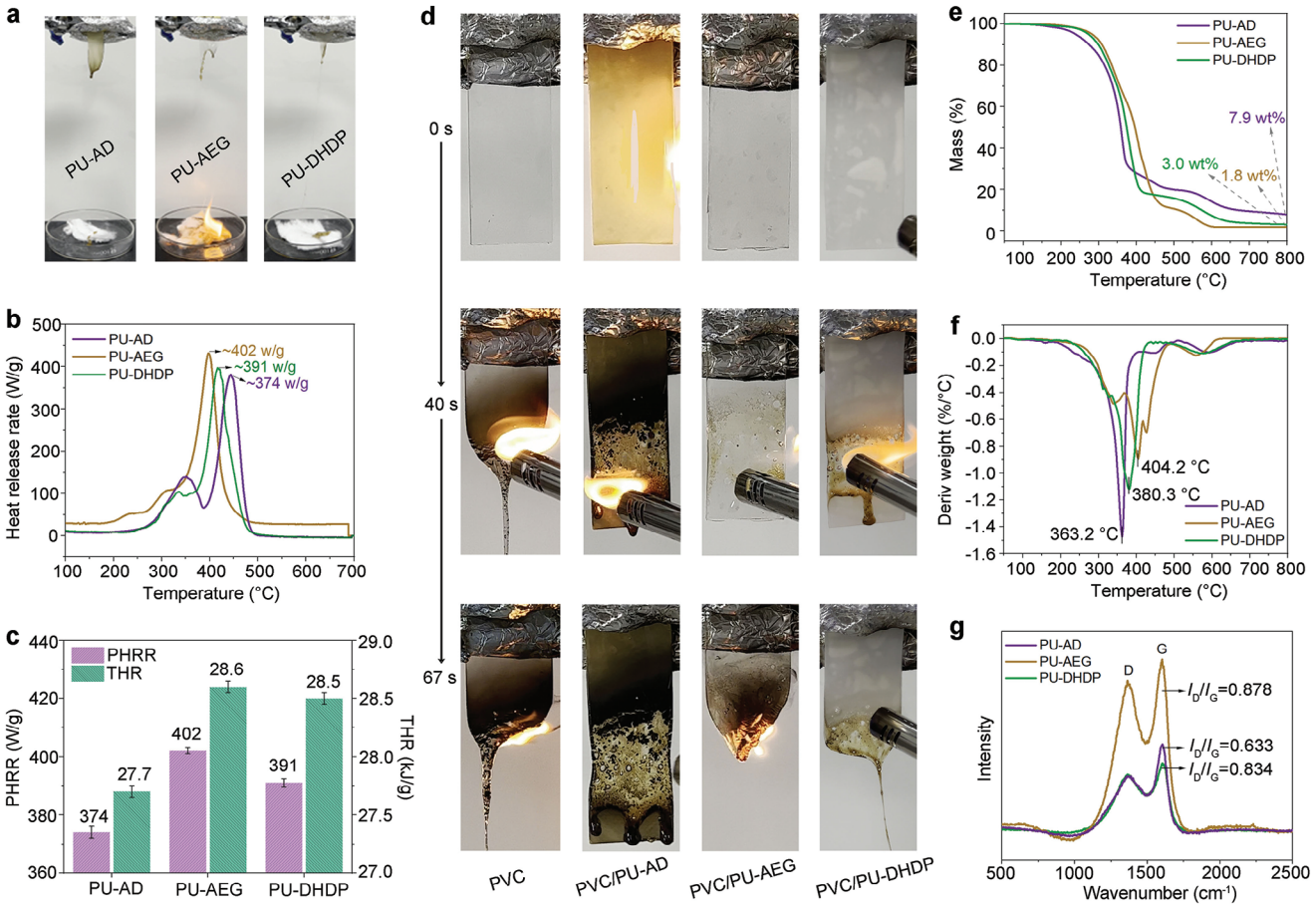

Figure 3. Intrinsic fire retardancy. a) Fire behavior of PU elastomers when igniting. b) HRR curves and c) PHRR and THR values of PU elastomers. d) Fire behavior of PU elastomers adhered to PVC substrate. e) TGA and f) DTG curves of PU elastomers. g) Raman spectra of char residues for PU elastomers.

2.4. Fire-Retardant Properties

It has been reported that phenanthrene ring-containing rosin derivatives have a good char-forming properties and high thermal stability, in addition to large steric hindrance. These features can significantly suppress the displacement and rearrangement of other chains in the polymer and thereby reduce the generation of combustible degradation products.[20] Thus, APA groups are anticipated to create a synergistic fire-retardant effect with DHDP groups in PU-AD. As-prepared PU elastomers strips were ignited to investigate their combustion behaviors (**Figure 3**a). Because all tested PU samples are thin films, a large portion of them is burned after ignition. Three samples can self-extinguish immediately after removing the flame. Compared with PU-AEG, the melting drops of PU-AD and PU-DHDP do not ignite the cotton, which is ascribed to the fire-retardant effect of phosphorus-containing moiety (Figure 3a; Videos S1–S3 and Table S6, Supporting Information). The better fire retardancy of PU-AD than PU-AEG and PU-DHDP is also reflected by its less melting drops and slower combustion rate. This suggests that the fire retardancy can be significantly improved by combining APA with DHDP. Microscale combustion calorimetry (MCC) was used to further evaluate the fire-retardant performances of PU elastomers. Both peak of heat release rate (PHRR) and total heat release (THR) values are in the order of PU-AD < PU-DHDP < PU-AEG, further demonstrating the low flammability of PU-AD (Figure 3b,c). When PU-AD is ignited, free radical reactions happen and a large amount of oxygen and heat is produced, thus sustaining the intense combustion of the matrix. Because both the PHRR and THR values are reduced due to the fire-retardant effect, the flammability of PU-AD can be restrained. Therefore, the lower values of PHRR and THR, the lower flammability of PU-AD.

Since adhesives are also used as coatings when adhered to substrates on larger scale,[16] we expanded the application of PU-AD as a fire protection coating for PVC substrate (Figure 3d). The PVC sheet (2 mm in thickness) is easily ignited and continues to burn after 60 s accompanied by severe melt-dripping, showing its high flammability due to the inclusion of plasticizers. In contrast, the PU-AD coated PVC sheet will self-extinguish immediately without dripping while maintaining structural integrity. The coated PVC sheets with PU-AEG or PU-DHDP exhibit a reduced fire damage length at earlier times than untreated PVC, but the underlying PVC does not retain its structural integrity. These results suggest that PU-AD adhesive can serve as an effective fire protective coating on flammable substrates.

To probe the fire-retardant mechanism of PU elastomers, thermogravimetric analysis (TG) was used to study their thermal

decomposition and char-forming abilities in the condensed phase. Both the initial decomposition temperature (T_i) and maximum thermal decomposition temperature (T_{max}) are in the order of PU-AD < PU-DHDP < PU-AEG, suggesting high thermal stability of APA in PU-AEG and earlier decomposition of DHDP in PU-DHDP (Figure 3e,f; Table S7, Supporting Information). Meanwhile, the earlier decomposition of DHDP can facilitate the decomposition and charring of APA, thus leading to the early decomposition of PU-AD and a higher char yield of 7.9 wt% at 800 °C, which is more than twice of PU-DHDP and fourfold greater than PU-AEG. Such a high char residue contributes to the good fire performance of PU-AD. The Raman spectra show a higher degree of graphitization of the char for PU-AD when compared with PU-DHDP and PU-AEG (Figure 3g). In addition, PU-AD generates a smooth, intact, and inflated char without cracks whereas PU-AEG and PU-DHDP leave split and cracked char residues after burning testing, indicative of the higher quality of the char from PU-AD (Figure S14, Supporting Information). PU-AD shows a more char residue and its char residue has a higher degree of graphitization, so the high-quantity and high-quality char can serve as a better physical barrier to protect the underlying substrate, thus improving the fire retardancy of PU-AD.

In addition to the charring effect in the condensed phase, the presence of nitrogen and phosphorus are often believed to have a role to play in inhibiting combustion in the gas phase, and so the evolved gaseous pyrolysis products of PUs with DHDP groups were investigated.[21] Despite no significant difference in pyrolysis products (Figures S15 and S16, Supporting Information), the absorption intensity of the products from PU-AD is significantly lower than those of PU-DHDP and PU-AEG, suggesting an inhibitory effect of AD groups on PU-AD. PU-AD shows stronger characteristic C═O peaks than PU-DHDP and PU-AEG, which can be ascribed to the formation of more C═O containing products (Figure S16, Supporting Information). In addition, both P- and N-containing products are detected in the pyrolysis of PU-AD (Figure S17, Supporting Information), and are likely to evolve into PO free radicals and N-containing gases (e.g., NH_3 or N_2), which can scavenge active free radicals (H•, OH•), while diluting fuels and oxygen, thus slowing the combustion process.[22] Therefore, it is the synergistic effect between APA and DHDP groups that work cooperatively in dual phases to contribute to the good fire performance of PU-AD.

2.5. Dual-Mode Degradability

In theory, the PU-AD and PU-AEG elastomers are expected to possess biodegradability because of the presence of labile ester bonds in their main chains.[23] To verify this, PU-AD, PU-AEG, and PU-DHDP films with a size of 10 × 10 × 0.2 mm^3 were immersed in 1.0 wt% aqueous solutions of lipase (**Figure 4a**). Both PU-AD and PU-AEG are substantially swollen with distorted shapes whereas PU-DHDP is virtually unchanged after 7 days. The PU-AD mixture becomes cloudier than PU-AEG after 30 days, demonstrating its faster biodegradation. After 180 days of immersion, PU-AD is almost completely dissolved while PU-DHDP remains intact, indicating the efficient biodegradability of PU-AD. The degradation products were measured by mass spectrometry and ion peaks at mass-to-charge ratios (m/z) of 279.3, 300.5, 373.2, and 540.1 are attributed to smaller species cleaved from ester groups in PU-AD due to the action of lipase (Figure S18, Supporting Information). These species disperse rather than dissolve in water, which produces cloudy suspension.

The chemical degradation of PU-AD in acetic acid solution was investigated since the ester groups and carbamates in its chemical structure are prone to degradation in acidic conditions.[24] After 7 days, the surface of PU-AD is rough, due to acid catalyzed degradation (Figure 4b). The degradation products were collected by evaporation of solvent with the residue analyzed by IR (Figure 4c). The appearance of a characteristic peak at 1695 cm^{-1} is ascribed to the C═O stretching vibration of COOH groups, indicating the decomposition of PU-AD ester groups. In contrast, the intensity of the characteristic C═O stretching vibration in COO groups at 1723 cm^{-1} is less intense, showing the incomplete decomposition of PU-AD after 7 days. After 90 days, the characteristic peak of COO groups almost completely disappears, implying complete degradation of ester groups. Meanwhile, the chemical cleavage of ester bonds of PU-AD in the presence of acetic acid was further confirmed by analysis of its degraded fragments (Figure 4d). Specifically, the mass-to-charge ratio (m/z) at 263.2, 299.4, 373.1, 440.3, and 562.6 are attributed to ion peaks ($[A + Na]^+$, B, $[C + H]^+$, D, $[A + B + Na]^+$), respectively, which are consistent with IR results. This also means that the degradation rate of PU-AD is faster in acid solution than in lipase solution, and the degradation products tend to dissolve in acid aqueous solution, suggesting a better degradability of PU-AD by way of chemical rather than biological methods. This can be attributed to the greater size of the enzyme which is sterically hindered from accessing binding sites necessary for action.

2.6. Application as Heat Dissipater Adhesives

PU-AD exhibits strong adhesion to copper substrates (Figure 2g), and so can be an ideal adhesive for copper electrical components. A heat dissipation film for thermal management was prepared by bonding copper powder with PU-AD. To demonstrate its practical cooling efficiency as a thermal interface material for computer CPU's, we applied as-prepared Cu/PU-AD coatings to a typical computer heat sink (see the preparation process in **Figure 5a** and Section 1.4 Supporting Information). We first mixed Cu powder and PU-AD at a mass ratio of 1:1 with the aid of ethanol (solid content of 20 wt%),[25] and then the Cu/PU-AD slurry was spread onto the CPU of a desktop computer and left to fully dry. The as-prepared Cu/PU-AD film achieves a satisfactory thermal conductivity (λ) of 3.50 W m^{-1} K^{-1} without electroconductibility. Since the thermal conductivity of PU-AD is as low as 0.12 W $m^{-1}K^{-1}$ (Table S8, Supporting Information) and nearly does not show a heat dissipation capacity (Figure S19, Supporting Information), the heat dissipation capacity of Cu/PU-AD is mainly due to copper powder of high thermal conductivity. For comparison, two commercial silicones, GD450 and Shin-Etsu 7921 which have λ values of 1.53 and 6.00 W m^{-1} K^{-1}, respectively, were used to compare thermal sink films under CPU overloading (Figure S20. Supporting Information).

To visually observe the heat dissipation capacity, infrared thermal imaging was employed to monitor the change in surface temperature of the CPU after the onset of overload operation

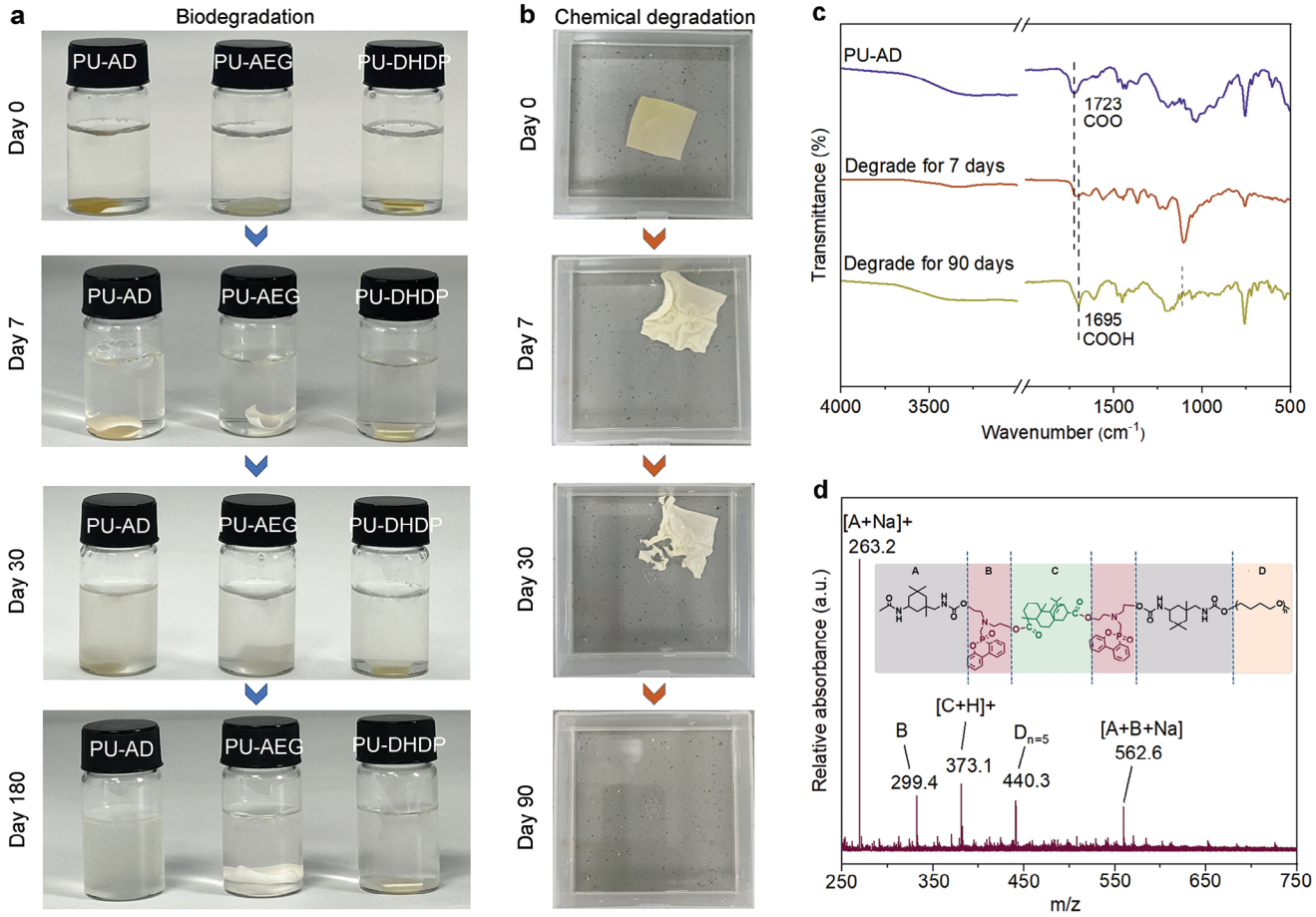

Figure 4. Dual-mode degradability of PU-AD. a) The biodegradation process of PU-AD, PU-AEG, PU-DHDP (0.5 g PU in lipase/water (0.2 g/20 g)). b) The chemical degradation process of PU-AD (1 g PU-AD in edible white vinegar (7 g/100 g)). c) IR spectra and d) MALDI-TOF/TOF results for degradation products of PU-AD after degraded in edible white vinegar for 90 days.

(from 0 to 120 s) (see Figures 5b,c and S21 and Videos S4–S7, Supporting Information). The surface temperature of the blank CPU increases rapidly from 16.5 to 85.2 °C after 120 s of overloading (Figure 5c). In comparison, upon being covered by commercial silicone GD450, the temperature of CPU is reduced within 10 °C, i.e., $\Delta T \leq 10$ °C (Figure 5b), and silicone Shin-Etsu 7921 ($\lambda = 6.0$ W m^{-1}K^{-1}) reduces the temperature of CPU more significantly, as reflected by a $\Delta T > 20$ °C as compared to the blank CPU. In sharp contrast, the surface temperature of CPU coated with Cu/PU-AD shows a ΔT of ≈18 °C at 60 s and ≈33 °C at 90 s, followed by a stable ΔT of ≈30 °C at 120 s, clearly demonstrating better heat dissipation performance of the Cu/PU-AD film. Although our Cu/PU-AD shows a smaller λ value (3.50 W m^{-1}K^{-1}) than Shin-Etsu 7921 (Figure 5b; Table S8, Supporting Information), it shows a better thermal dissipation capability than the later particular after 40 s, which is primarily ascribed to the formation of a more even and thinner Cu/PU-AD film than the commercial silicone. In addition, we further tested the heat dissipation performance of a Cu/PU-AD film on laptop computer. The results show that the back temperature of laptop during operation was reduced from ≈40 to ≈32 °C for the Shin-Etsu 7921 coating, whereas the temperature is reduced to ≈25 °C for the Cu/PU-AD film (Figure S22, Supporting Information), further highlighting the improved heat dissipation ability of Cu/PU-AD.

Due to the good solubility of PU-AD in ethanol, the PU-AD can be fully recovered from used Cu/PU-AD mixtures by dissolving it in ethanol under stirring and ultrasonic treatment followed by centrifugation (Figure 5d). In comparison, two commercial silicones cannot be recovered or reused due to their cross-linked structures. This further demonstrates the advantage of as-created PU-AD elastomer adhesives over existing silicone-based counterparts, and thus its application can help reduce waste plastic and microplastic pollution.

3. Conclusion

In summary, we have successfully synthesized a robust, fire-retardant, switchable sustainable polyurethane adhesive by rationally designing a unique hard segment combining APA and DOPO moieties for PU. Because of the combination of the polar structure of acrylic pimaric acid with H-bonding and π–π stacking, the PU elastomer exhibits a superhigh adhesion force of 38.8 N cm^{-1} with PVC as substrate, and can be reused without adhesion loss using ethanol exhibiting an on-demand debonding ability. In addition, the PU adhesive can quickly self-extinguish

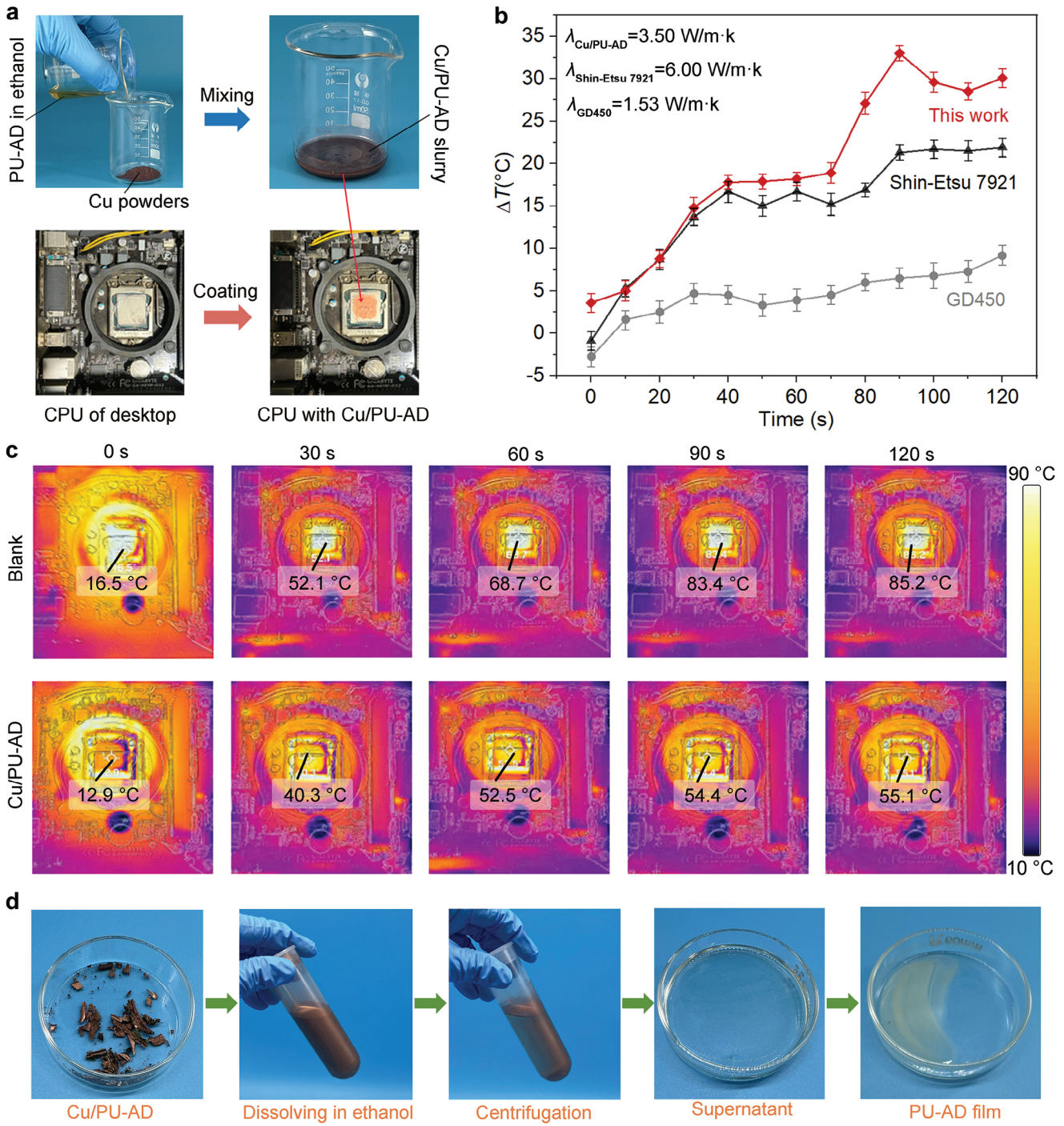

Figure 5. Heat dissipation of Cu/PU-AD. a) The preparation process of Cu/PU-AD slurry and digital images of CPU after coated with Cu/PU-AD. b) Temperature changes of CPU after overloading with two commercial silicones and Cu/PU-AD, ΔT is the temperature difference between blank CPU and CPU coated with commercial silicones and Cu/PU-AD after overloading, respectively. c) Infrared thermal images before and after overloading with Cu/PU-AD. d) The extraction process of PU-AD from Cu/PU-AD film.

once ignited and thus can effectively protect the underlying substrate from fire damage, due to the dual-phase modes of action of the AD hard segments derived from the synergism between APA and DOPO components. The designed PU-AD is both biodegradable and chemically degradable due to multiple ester bonds in the main chain. The PU elastomers show great potential as a reliable and recyclable adhesive for Cu-based heat dissipaters for thermal management of electronics. This work offers an innovative design approach for next-generation functional sustainable adhesives that are expected to find extensive applications

particularly for electronics. However, much work needs to be done to achieve the scalable production of PU-AD adhesives and to further improve the functionalities for realizing the practical application, e.g., in harsh environments.

Supporting Information

Supporting Information is available from the Wiley Online Library or from the author.

Acknowledgements

This work acknowledged the financial support of the National Natural Science Foundation of China (Grant Nos. 32301545; 32071712), the China Postdoctoral Foundation (Grant No. 2023M733779), and the Australian Research Council (Grant Nos. FT190100188, LP230100278, DP240102628, DP240102728).

Open access publishing facilitated by University of Southern Queensland, as part of the Wiley - University of Southern Queensland agreement via the Council of Australian University Librarians.

Conflict of Interest

The authors declare no conflict of interest.

Data Availability Statement

The data that support the findings of this study are available in the supplementary material of this article.

Keywords

biodegradation, fire retardancy, heat dissipater, peel strength, polyurethane adhesive

Received: May 27, 2024
Revised: August 8, 2024
Published online:

[1] a) H. Fan, J. P. Gong, *Adv. Mater.* **2021**, *33*, 2102983; b) S. Nam, D. Mooney, *Chem. Rev.* **2021**, *121*, 11336.
[2] a) P. Dwivedi, K. Singh, K. Chaudhary, R. Mangal, *ACS Appl. Polym. Mater.* **2022**, *4*, 4588; b) R. Pinnaratip, M. S. A. Bhuiyan, K. Meyers, R. M. Rajachar, B. P. Lee, *Adv. Healthcare Mater.* **2019**, *8*, 1801568; c) Y. Lv, F. Cai, X. Zhao, X. Zhu, F. Wei, Y. Zheng, X. Shi, J. Yang, *Adv. Funct. Mater.* **2024**, *34*, 2314402.
[3] a) H. Wu, H. Wang, M. Luo, Z. Yuan, Y. Chen, B. Jin, W. Wu, B. Ye, H. Zhang, J. Wu, *Mater. Horiz.* **2024**, *11*, 1548; b) W. Zeng, Y. Jin, R. Zhou, Y. Li, H. Chen, *Chem. Eng. J.* **2024**, *482*, 148994.
[4] a) T. Tirri, M. Aubert, C. E. Wilén, R. Pfaendner, H. Hoppe, *Polym. Degrad. Stabil.* **2012**, *97*, 375; b) W. Y. Chang, Y. W. Pan, C. N. Chuang, J. J. Guo, S. H. Chen, C. K. Wang, K. H. Hsieh, *J. Polym. Res.* **2015**, *22*, 243.
[5] C. Cai, Q. Sun, K. Zhang, X. Bai, P. Liu, A. Li, Z. Lyu, Q. Li, *Fire Mater.* **2022**, *46*, 130.
[6] Y. Xue, J. Lin, T. Wan, Y. Luo, Z. Ma, Y. Zhou, B. T. Tuten, M. Zhang, X. Tao, P. Song, *Adv. Sci.* **2023**, *10*, 2207268.
[7] Y. Xue, T. Zhang, H. Peng, Z. Ma, M. Zhang, M. Lynch, T. Dinh, Z. Zhou, Y. Zhou, P. Song, *Nano Res.* **2024**, *17*, 2186.
[8] H. Ding, C. Xia, J. Wang, C. Wang, F. Chu, *J. Mater. Sci.* **2016**, *51*, 5008.
[9] F. Wang, Z. Yang, J. Li, C. Zhang, P. Sun, *ACS Macro Lett.* **2021**, *10*, 510.
[10] a) H. Y. Mi, X. Jing, B. N. Napiwocki, B. S. Hagerty, G. Chen, L. S. Turng, *J. Mater. Chem. B* **2017**, *5*, 4137; b) A. S. Al Hosni, J. K. Pittman, G. D. Robson, *Waste Manage.* **2019**, *97*, 105.
[11] a) B. Liu, T. Guan, G. Wu, Y. Fu, Y. Weng, *Polymers* **2022**, *14*, 1515; b) H. Wang, D. Wei, A. Zheng, H. Xiao, *Polym. Degrad. Stabil.* **2015**, *116*, 14.
[12] a) M. Sun, Y. Yang, M. Huang, S. Fu, Y. Hao, S. Hu, D. Lai, L. Zhao, *Sci. Total Environ.* **2022**, *807*, 151042; b) J. Qi, J. Wu, J. Chen, H. Wang, *Polym. Degrad. Stabil.* **2019**, *160*, 229.
[13] a) M. Shen, R. Almallahi, Z. Rizvi, E. Gonzalez-Martinez, G. Yang, M. L. Robertson, *Polym. Chem.* **2019**, *10*, 3217; b) G. Dai, Q. Xie, C. Ma, G. Zhang, *ACS Appl. Mater. Interfaces* **2019**, *11*, 11947.
[14] a) T. Nogusa, C. B. Cooper, Z. Yu, Y. Zheng, Y. Shi, Z. Bao, *Matter* **2023**, *6*, 2439; b) Y. Zhang, S. Zhang, F. Sun, Q. Ji, J. Xu, B. Yao, Z. Sun, T. Liu, G. Hao, Y. Hu, G. Zhang, W. Jiang, J. Fu, *Adv. Funct. Mater.* **2023**, *33*, 2304653; c) L. Liu, H. Deng, W. Zhang, S. A. Madbouly, Z. He, J. Wang, C. Zhang, *ACS Sustainable Chem. Eng.* **2021**, *9*, 147; d) X. Li, J. Ke, J. Wang, M. Kang, Y. Zhao, Q. Li, C. Liang, *J.CO2 Util.* **2019**, *31*, 198; e) H. Wang, X. Li, E. Zhang, J. Shi, X. Xiong, C. Kong, J. Ren, C. Li, K. Wu, *Langmuir* **2023**, *39*, 17611; f) J. Li, L. Zhao, C. Hong, M. Liu, Y. Wang, Y. Song, R. Zhai, J. Zhang, C. Zhou, *Prog. Org. Coat.* **2024**, *186*, 108018; g) Y. Li, S. Chen, J. Shen, S. Zhang, M. Liu, R. Lv, W. Xu, *Appl. Sci.* **2021**, *11*, 4784; h) R. Li, J. A. Ton Loontjens, Z. Shan, *Eur. Polym. J.* **2019**, *112*, 423; i) H. Ming, C. Tian, N. He, X. Zhao, F. Luo, Z. Li, J. Li, H. Tan, Q. Fu, *Polym. E.* **2022**, *33*, 1811; j) X. Liu, J. Zhao, X. Lin, *J. Appl. Polym. Sci.* **2022**, *139*, 52122; k) Z. Yildiz, A. Onen, A. Gungor, *J. Adhes. Sci. Technol.* **2016**, *30*, 1765; l) M. Fuensanta, A. Khoshnood, F. Rodríguez-Llansola, J. M. Martín-Martínez, *Materials* **2020**, *13*, 627.
[15] J. Wang, C. Shi, N. Yang, H. Sun, Y. Liu, B. Song, *Compos. Struct.* **2018**, *184*, 1189.
[16] Z. H. Wang, B. W. Liu, F. R. Zeng, X. C. Lin, J. Y. Zhang, X. L. Wang, Y. Z. Wang, H. B. Zhao, *Sci. Adv.* **2022**, *8*, add8527.
[17] Q. Zhao, M. Zhang, S. Gao, Z. Pan, Y. Xue, P. Jia, C. Bo, Z. Luo, F. Song, Y. Zhou, *J. Mater. Chem. A* **2022**, *10*, 11363.
[18] L. Chen, H. B. Zhao, Y. P. Ni, T. Fu, W. S. Wu, X. L. Wang, Y. Z. Wang, *J. Mater. Chem. A* **2019**, *7*, 17037.
[19] S. Dai, L. Gao, F. Yan, J. Guo, Y. Zhao, Y. Liu, L. Liu, Y. Ao, *Compos. Commun.* **2023**, *38*, 101498.
[20] L. Zhang, Y. Jiang, Z. Xiong, X. Liu, H. Na, R. Zhang, J. Zhu, *J. Mater. Chem. A* **2013**, *1*, 3263.
[21] a) Y. Xue, J. Feng, Z. Ma, L. Liu, Y. Zhang, J. Dai, Z. Xu, S. Bourbigot, H. Wang, P. Song, *Mater. Today Phys.* **2021**, *21*, 100568; b) Y. Xue, Z. Ma, X. Xu, M. Shen, G. Huang, S. Bourbigot, X. Liu, P. Song, *Compos. Part A–Appl. S.* **2021**, *144*, 106317; c) Y. Xue, T. Zhang, L. Tian, J. Feng, F. Song, Z. Pan, M. Zhang, Y. Zhou, P. Song, *Chem. Eng. J.* **2023**, *472*, 144986; d) Y. Xue, T. Zhang, L. Tian, J. Feng, F. Song, Z. Pan, G. Huang, M. Zhang, Y. Zhou, P. Song, *Int. J. Biol. Macromol.* **2024**, *265*, 130790.
[22] a) Y. Xue, M. Shen, Y. Zheng, W. Tao, Y. Han, W. Li, P. Song, H. Wang, *Compos. Part B–Eng.* **2020**, *183*, 107695; b) Y. Xue, J. Feng, S. Huo, P. Song, B. Yu, L. Liu, H. Wang, *Chem. Eng. J.* **2020**, *397*, 125336.
[23] Y. Xu, S. Sen, Q. Wu, X. Zhong, R. H. Ewoldt, S. C. Zimmerman, *Chem. Sci.* **2020**, *11*, 3326.
[24] X. Xun, X. Zhao, Q. Li, B. Zhao, T. Ouyang, Z. Zhang, Z. Kang, Q. Liao, Y. Zhang, *ACS Nano* **2021**, *15*, 20656.
[25] C. Zhang, Y. Tang, T. Guo, Y. Sang, D. Li, X. Wang, O. J. Rojas, J. Guo, *InfoMat* **2024**, *6*, e12466.